Journal of Metastable and Nanocrystalline Materials
ISSN: 2297-6620, Vol. 40, pp 1-13
doi:10.4028/p-M0pMsg

Submitted: 2024-01-21
Revised: 2024-04-06
Accepted: 2024-04-10
Online: 2024-08-19

Characterization and Properties of ZnO:Nd^{3+} Nanomaterial Synthesized by Chemical Synthesis Method

Sudha Pal[1,a], Jitendra Pal Singh[2,b], Yogesh Kumar Sharma[3,c], Atanu Nag[2,d] , Shu-Chi Huang[4,e] and Shyan-Lung Chung[5,f]

[1]Department of Physics, M.B. Govt. P.G. College, Haldwani, Uttrakhand, India-263139

[2]Department of Physics, School of Sciences, IFTM University, Moradabad, India-244102

[3]Department of Physics, Sri Dev Suman Uttarakhand University, Pt. L.M.S. Campus, Rishikesh (Dehradun), Uttarakhand, India-249201

[4]Department of Applied Chemistry, National Chaiyi University, 60004, Chiayi, Taiwan, ROC

[5]Department of Chemical Engineering, National Cheng Kung University, 70101, Tainan, Taiwan, ROC

[a]palsudh2011@gmail.com, [b]paljitendra124@gmail.com, [c]dryksharma@yahoo.com, [d]tnnag79@gmail.com, [e]nkcu77@gmail.com, [f]slchung@mail.ncku.edu.tw

Keywords: Nanostructure, Nanoparticle, Nanomaterial, Optoelectronic Nanomaterial.

Abstract. Nd^{3+} ion-doped ZnO nanomaterial was prepared using chemical synthesis method and its fluorescence spectra have been investigated at room temperature. From SEM images of the synthesized ZnO: Nd^{3+} nanoparticles it is observed that an increase in concentration of Nd^{3+} ions leading to the decrease in the particle size. Nearly hexagonal shapes for the dark spots in the SAED images indicate that the ZnO nanoparticles are almost hexagonal. The oscillator strengths leading to 4f ↔ 4f transitions are characterized by different Judd-Ofelt intensity parameters Ω_λ (λ = 2, 4 and 6). These Ω_λ parameters along with the fluorescence data and various radiative properties viz., spontaneous emission probability (A), radiative life time (τ), fluorescence branching ratio (β) and stimulated emission cross-section (σ_p) were evaluated and compared with the reported values. The values of these parameters indicate that the observed transitions $^4F_{3/2} \rightarrow {}^4I_{11/2}$, $^4F_{3/2} \rightarrow {}^4I_{13/2}$ and $^4F_{3/2} \rightarrow {}^4I_{15/2}$ can be considered to be good laser transitions in the near infrared region for different optoelectronic and spintronic uses.

Introduction

Tripositive lanthanide ions exhibit unique spectroscopic properties [1]. Rare earth (RE)-lanthanide ions are improved glowing resources owing to their strong emission resulting from their 4f intra-shell changes [2]. Due to tight shielding of 4f shells by the 5s and 5p shells, the ligand surroundings develops weak influence on the electronic clouds of these ions. But still, this weak perturbation is effectively responsible for the developed fine spectral structure. The absorption spectra of lanthanide ions doped into single crystal show many fine line groups, producing an atomic spectrum. In the case of lanthanide doped glasses, Judd-Ofelt (J-O) intensity parameters [3] are very useful in the calculation of laser parameters like the spontaneous emission probability (A), fluorescence branching ratio (β), radiative life time (τ) and stimulated emission cross-section (σ_p), which are used to predict laser action of various transitions in doped nanomaterial.

The laser parameters are used in prediction of laser action in different doped glass specimens. On the other hand, oxide materials are the materials which have organic strength and current constancy from top to bottom. Among oxide material, zinc oxide (ZnO) and cadmium sulfide (CdS) are the two most important hosts which have been used extensively in the fabrication of lasers and amplifiers. As compared to other material, at the excitation and lasing wavelengths, the ZnO nanomaterials have superior optical clarity.

So, additionally, they are well-matched with the construction development during the growth of photosensitive materials. Looking at the importance of ZnO nanomaterial it was believed to be

worthwhile to plan a new kind of lanthanide doped ZnO nanomaterial to carry out its photosensitive aspects by studying its fluorescence bands.

This information is also highly required while developing new optical devices. Several reports are available on the synthesis and studies of the luminescent properties of doped semiconductors in various morphologies [4, 5]. Many information are obtainable on combination and revisions of luminescent properties with other RE ions [2]. Neodymium (Nd) doping in ZnO films was found to enhance their photo-catalytic and anti-bacterial activities [4]. Nd is typically 10-18% of the RE elements and is comfortable with marketable deposits from the luminosity RE element minerals bastnäsite and monazite [3]. Nd is exclusive of the most generally used essentials for great control laser actions. Moreover, Nd^{3+} doping reduces the band gap energy [6] and enhances the possibility of the photo-degradation of organic dyes under visible light as well as under UV light. The RE component drugged ZnO:Nd^{3+} nanoparticle finds numerous attractive possessions in optoelectronic and spintronic uses. Current study presented the synthesis and studies of the ZnO doped with 0.1 mol%, 0.2 mol% and 0.3 mol % Nd^{3+} ion [5].

This paper will mainly aim to discuss about the method synthesis of Nd^{3+} ion-doped ZnO (ZnO:Nd^{3+}) nanomaterial and its fluorescence spectra at room temperature. Transmission electron microscopy (TEM), scanning electron microscopy (SEM) and selected area electron diffraction (SAED) imageries of the synthesized sample are utilized to explain the change in morphology of the ZnO:Nd^{3+} nanoparticles with the varying Nd^{3+} ion concentrations. It will also discusses about the oscillator strengths corresponding to 4f ↔ 4f transitions as characterized by different J-O intensity parameters (Ω_λ). These parameters along with the fluorescence data and various radiative properties viz., spontaneous emission probability (A), radiative life time (τ), fluorescence branching ratio (β) and stimulated emission cross-section (σ_p) were evaluated and compared with the reported values. The values of these parameters indicate that the observed transitions $^4F_{3/2} \rightarrow {}^4I_{11/2}$, $^4F_{3/2} \rightarrow {}^4I_{13/2}$ and $^4F_{3/2} \rightarrow {}^4I_{15/2}$ can be considered to be good laser transitions in the near infrared region for different optoelectronic and spintronic uses.

Materials and Methods

In this study, ZnO:Nd^{3+} nanomaterial was prepared using chemical synthesis method [1, 7]. All the solvents, viz. iso-propanol, ethanol, glycerol, methanol and acetone were of analytical research (AR) grade and 99.99% pure and these were used as received without further purification. Initially, the ZnO nanoparticles were stirred in alcoholic media like ethanol, methanol or propanol. In intoxicating alcoholic media growth of oxide units is found to be relaxed and it is convenient [2, 8]. Different solutions have been prepared by dissolving 0.2725 g of $ZnCl_2$ (10^{-1} M, 20 ml), 0.545 g NaOH (10^{-1} M, 100 ml) and glycerol in alcoholic media (ethanol). Glycerol solution is then slowly added to NaOH solution while it has been continuously stirred. The resulting solution has been stirred for one hour before adding $ZnCl_2$ and 0.1mol%, 0.2mol% and 0.3mol % Nd^{3+} ions solution to it. After two hours of constant stirring a milky white solution obtained. Size selective precipitation has been carried out using acetone as a non-solvent. The precipitate is then washed in methanol or ethanol followed by evaporation at room temperature to obtain ZnO: nanoparticles in white powder form. Fig. 1 illustrates the schematic overview of the synthesis workflow of ZnO:Nd^{3+} nanoparticles. Fluorescence bands for the developed ZnO:Nd^{3+} nanoparticles, strained in alcoholic mass media, were recorded at room temperature using Perkin Elmer Fluoroscence spectrophotometer (model LS50B) for the visible and near infrared (NIR) range. X-ray Diffraction spectra of the sample were recorded by Powder diffractometer (Model: X'pert Pro Powder diffractometer, Manufacturer: PANalytical, Country: Japan) SEM and TEM imageries are recorded by Scanning Electron Microscope (Model: FEI Quanta 200F, Manufacturer: FEI Company, Country: USA) and Transmission Electron Microscope (Model: FEI Technai G2200kV S-twin, Manufacturer: Aurora, Country: European University Alliance) respectively. Fourier Transform Infrared (FTIR) spectrum is obtained from PC using Omnic series software (Model: INQSOF018, Manufacturer: Thermo Fisher Scientific, Country: USA). Absorption spectra of the sample are

recorded by double beam spectrophotometer (Model: 2375, Manufacturer: Electronicsindia, Country: India) and Fluorescence spectra of the sample are recorded by Fluorescence Spectrophotometer (Manufacturer: Labindia Instruments, Model: F-4600, Country: India).

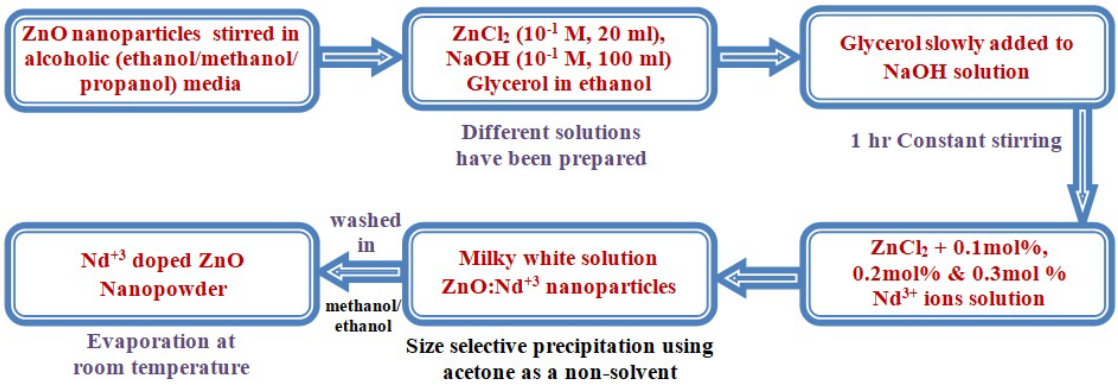

Fig. 1. Schematic illustration of the synthesis workflow of ZnO:Nd^{3+} nanoparticles

Results

X-Ray Diffraction (XRD) Typical XRD spectra of 0.1 mol% Nd^{3+} doped ZnO nanomaterial is shown in Fig. 2. The ZnO: Nd^{3+} nanopowder's crystalline size is estimated to be about 200-50 nm. The sharp diffraction bands at $2\theta^0 = 31.73^0$ have been observed for 0.1 mol% Nd^{3+} doped ZnO nanomaterial. The XRD patterns reveal well developed reflections of hexagonal wurtzite Zn, without any indications of the phases related with Nd or other impurities such as Nd_2O_3 etc. This finding implies that the Nd^{3+} ion doping most probably occurs by substituting Zn atoms in the crystal structure.

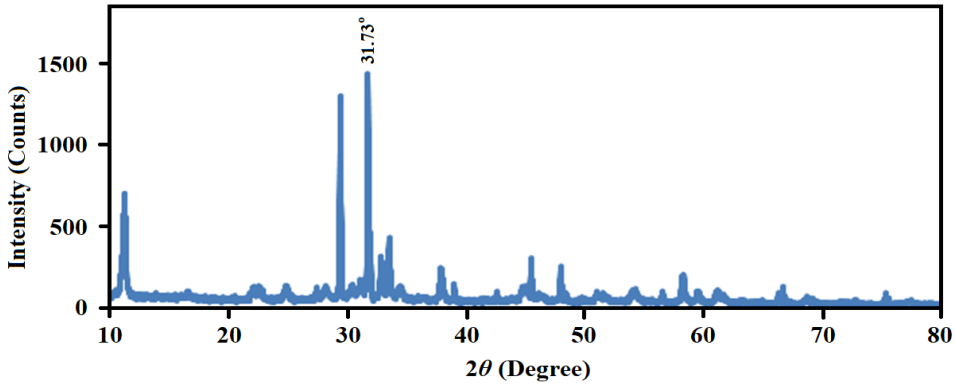

Fig. 2. XRD spectra of ZnO nanomaterial doped with 0.1 mol% of Nd^{3+} ion

Scanning Electron Microscopy (SEM). SEM images of the ZnO:Nd^{3+}-nanomaterials have been recorded at room temperature and shown in Fig. 3. The images shows creation of ZnO:Nd^{3+} nanostructures with well detached exposure but having gathered spots that are nearly circular in shape. These elements exhibit strong necking with their neighbors. The materials used were of varying sizes and are not homogeneous. The image shows approximate spherical shape of ZnO nanoparticles and the size of the particles are around 50-200 nm. It demonstrates clearly the formation of spherical ZnO: Nd^{3+} nanoparticles, and change of the morphology of the nanoparticles with the different concentration of Nd^{3+} ions. It is observed that with the increase in concentration of Nd^{3+} ions, the particle size decreases. Comparable behavior of ZnO nanomaterial doped with Pr^{3+} ion is also detected by Pal et al in recent past [9].

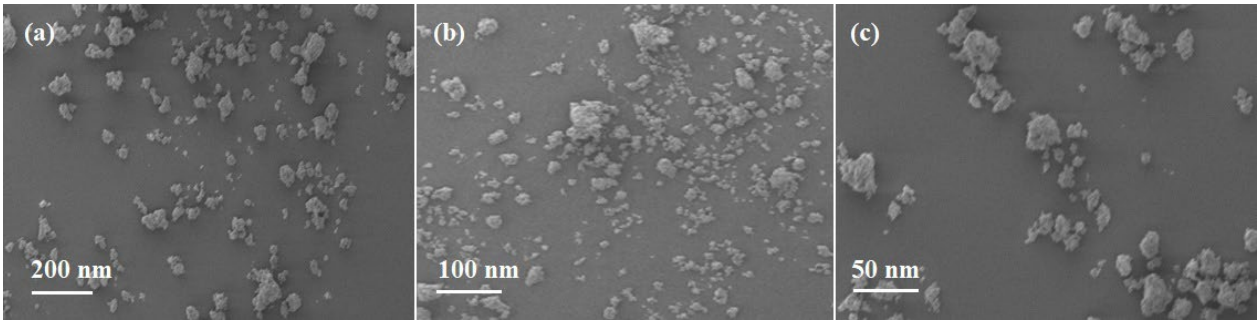

Fig. 3. SEM micrograph of ZnO nanomaterial doped with (a) 0.1 mol %, (b) 0.2 mol % and (c) 0.3 mol % concentration of Nd^{3+} ions

Transmission Electron Microscopy (TEM). TEM imagings and particular part of the electron spreading shapes of ZnO:Nd^{3+} nanoparticle have been recorded and is shown in Fig. 4. Nearly hexagonal shapes for the dark spots in the images indicate that the ZnO nanoparticles are almost hexagonal. Some regions of the sample can scatter or absorb electrons and seems to be darker, while some other regions that transmit electrons seem to be brighter. Here the transmitted (unscattered) electron beam is selected with the aperture, and the scattered beams are blocked. Since the unscattered beam is selected, region with high mass materials seems to be dark.

The estimated average particle size corresponding to 0.1 mol%, 0.2 mol% and 0.3 mol% Nd^{3+} ion doped ZnO nanoparticles are 200 nm, 100 nm and 50 nm respectively. When the concentration of Nd^{3+} is increased the particle size decreases and this is clearly seen in the TEM images. These results are also consistent with other RE metal doped ions like Gd doped ZnO nanomaterial [10].

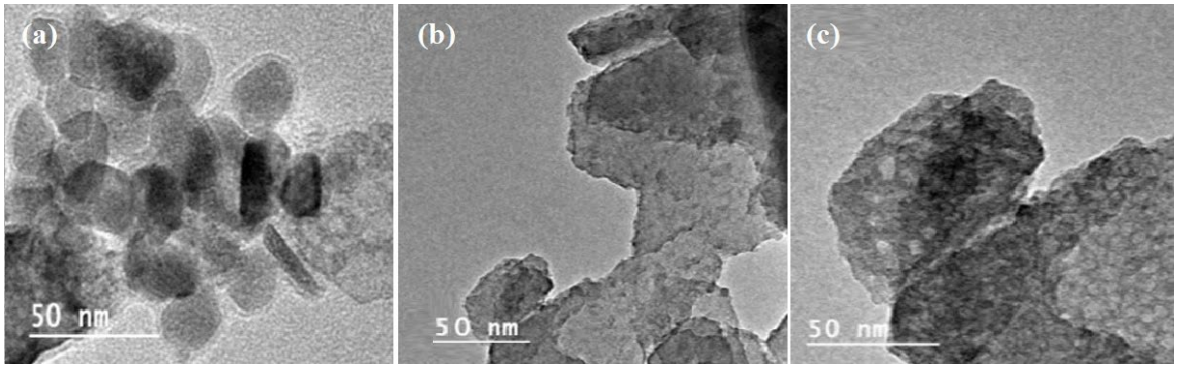

Fig. 4. TEM micrograph of ZnO nanomaterial doped with (a) 0.1 mol%, (b) 0.2 mol% and (c) 0.3 mol% of Nd^{3+} ion

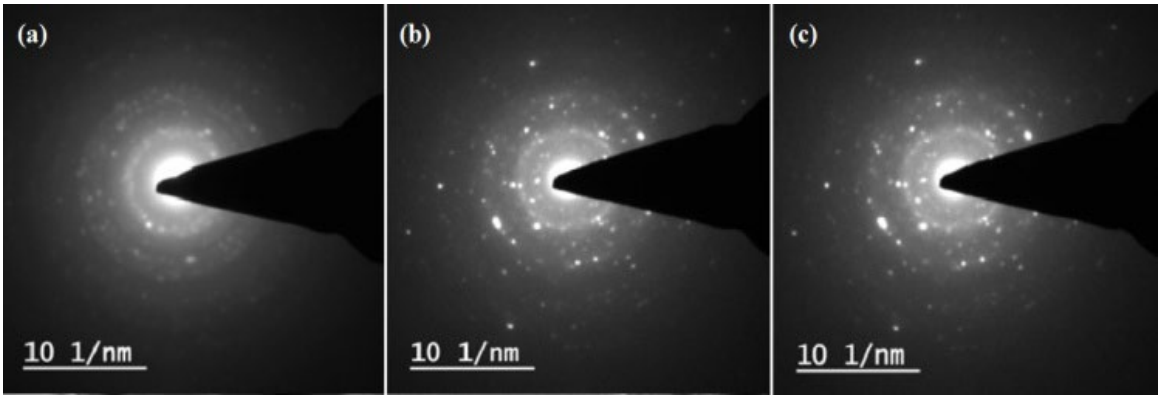

Fig. 5. High Resolution TEM showing Selected Area Electron Diffraction (SAED) pattern of ZnO nanomaterial doped with (a) 0.1 mol%, (b) 0.2 mol% and (c) 0.3 mol% of Nd^{3+} ion

High resolution TEM imageries showing selected area electron diffraction (SAED) pattern of ZnO:Nd^{3+} nanomaterial doped with 0.1 mol%, 0.2 mol% and 0.3 mol% of Nd^{3+} ion are respectively

shown in Fig. 5 (a), 5 (b) and 5 (c). SAED pattern of ZnO:Nd^{3+} nanomaterial consists of bright uniform rings confirming preferential orientation for nanocrystals instead of random orientation different concentration level. Nearly hexagonal shapes for the dark spots in the images indicate that the ZnO nanoparticles are almost hexagonal. The estimated average particle size corresponding to 0.1 mol%, 0.2 mol% and 0.3 mol% are 50 nm, 100 nm and 200 nm.

Fourier Transform Infra Red (FTIR) spectroscopy. The FTIR spectra of 0.1 mol% Nd^{3+} doped ZnO nanomaterial in Fig. 6 consists of numerous peaks which are broad and moderate in bandwidth.

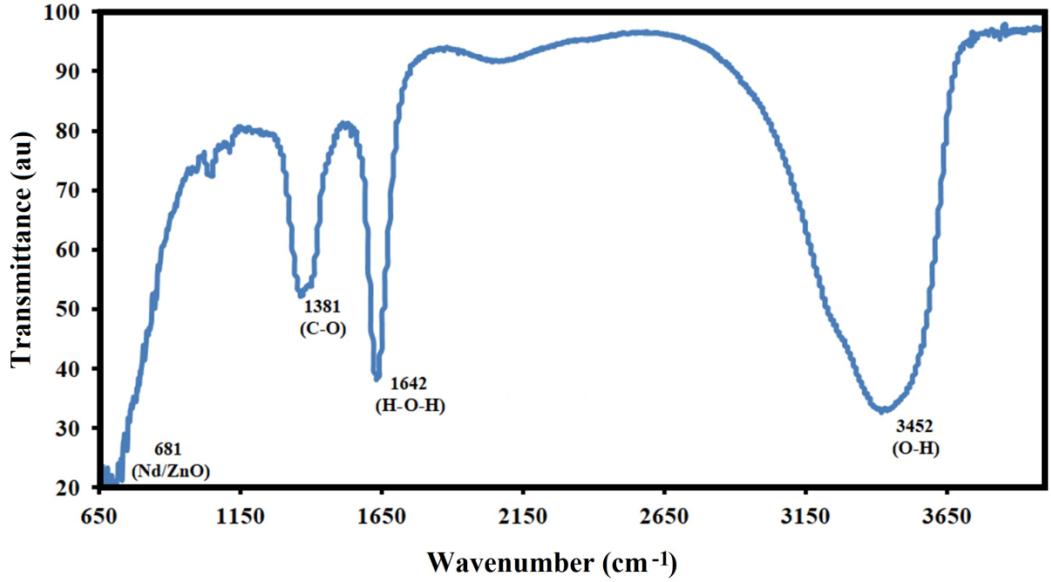

Fig. 6. FTIR spectra of ZnO nanomaterial doped with 0.1 mol% of Nd^{3+} ion

The absorption peak in the range 681 cm^{-1} are due to metal-oxygen bonds (Nd/ZNO). Absorption band at around 1381 cm^{-1} is due to the C-O stretching vibration of ethanol used for the synthesis [11-12]. The peak at 1642 cm^{-1} is assigned due to the bending vibrations of H-O-H bond. The broad band around 3452 cm^{-1} is equivalent to the basic stretching ambiance of O-H indicating the presence of hydrogen groups.

UV-Visible Absorption Spectra. Optical property of nanoparticles is an important property which gives specific information about the agglomeration state, concentration, size, shape, etc. near the surface of the particles. These particles interact with specific wavelength of light and show maximum absorption at a particular wavelength [13]. The intensities of absorption transitions are measured in terms of the probability for absorption of radiant energy (P_{exp}) which represents the number of classical oscillators present in one ion, more commonly referred to as the oscillator strength.

Table 1 gives the oscillator strengths for various absorption levels of 0.1 mol% Nd^{3+} doped ZnO nanomaterial. It is showing maximum for $^4I_{9/2} \rightarrow {}^4G_{5/2}, {}^2G_{7/2}$ transition.

The absorption spectra of different concentration Nd^{3+} ion doped ZnO nanomaterial have been presented in Fig. 7. The intensity of $^4I_{9/2} \rightarrow {}^4G_{5/2}, {}^2G_{7/2}$ transition is the principal determiners of the Ω_2. This transition satisfies the selection rule $|\Delta J| \leq 2$ and is known as hypersensitive transition. However, for a solid material the oscillator strengths is generally expressed in terms of line strength (S_{exp}).

Table 1. Oscillator strengths for various absorption levels of 0.1 mol% ZnO:Nd^{3+} nanomaterial

Absorption levels	Wavelength (λ nm)	Wave Number (1/ λ cm)	Oscillator strength (10^{-6})
$^4F_{5/2}$, $^2H_{9/2}$	824	12135	12.24
$^4F_{7/2}$, $^4S_{3/2}$	775	12903	13.81
$^4F_{9/2}$	682	14662	1.46
$^2H_{11/2}$	611	16366	0.98
$^4G_{5/2}$, $^2G_{7/2}$	591	16920	20.65
$^2K_{13/2}$, $^4G_{7/2}$	551	18115	9.55
$^4G_{9/2}$	540	18518	1.78
$^2K_{15/2}$, $^2G_{9/2}$, $^3D_{3/2}$	462	21645	2.99
$^4D_{3/2}$, $^4D_{5/2}$, $^1F_{1/2}$, $^4D_{1/2}$	377	26525	10.42

A good agreement is found between the calculated and experimental line strengths for various absorption levels of 0.1 mol% Nd^{3+} doped ZnO nanomaterial and it is given in Table 2. The group strengths, definite in affairs of line strength (S), signifies the absorption spectra ZnO:Nd^{3+} nanoparticles samples [14-15].

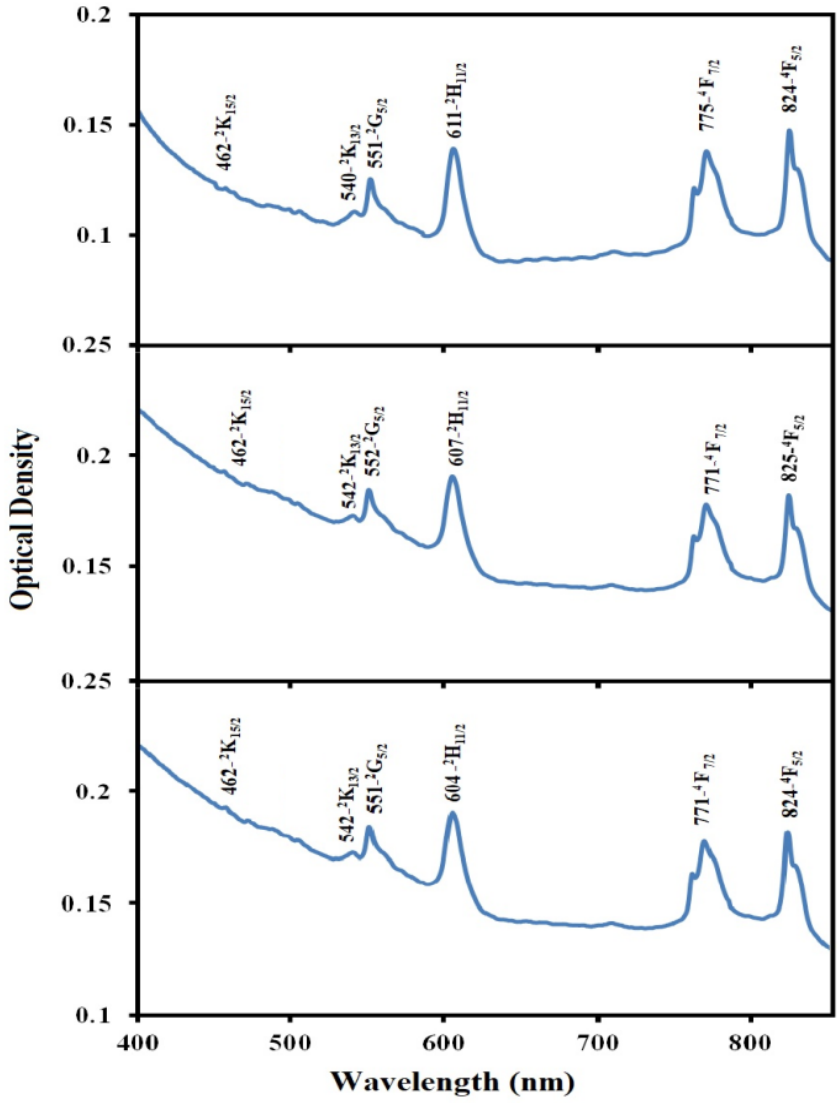

Fig. 7. Absorption spectra of 0.1 mol %, 0.2 mol % and 0.3 mol % Nd^{3+} ion doped ZnO nanomaterial

Table 2. Experimental (S_{exp}) and calculated (S_{cal}) line strengths with their differences (ΔS) for various absorption levels of 0.1 mol% Nd^{3+} doped ZnO nanomaterial

Absorption levels	S_{exp} (10^{-20})	S_{cal} (10^{-20})	ΔS
$^4F_{5/2}$, $^2H_{9/2}$	6.04	5.30	0.74
$^4F_{7/2}$, $^4S_{3/2}$	0.64	0.56	0.08
$^4F_{9/2}$	0.59	0.38	0.21
$^2H_{11/2}$	0.35	0.09	0.26
$^4G_{5/2}$, $^2G_{7/2}$	7.31	6.61	0.70
$^2K_{13/2}$, $^4G_{7/2}$	3.15	1.60	1.55
$^4G_{9/2}$	0.57	0.60	-0.03
$^2K_{15/2}$, $^2G_{9/2}$, $^3D_{3/2}$	0.82	0.66	0.16
$^4D_{3/2}$, $^4D_{5/2}$, $^1F_{1/2}$, $^4D_{1/2}$	2.35	1.82	0.53

Judd-Ofelt (J-O) Intensity Parameters. The oscillator strengths leading to 4f ↔ 4f transitions are characterized by the typical J-O intensity parameters (Ω_2, Ω_4 and Ω_6) [16]. This deviation of the line asset is mirrored in the values of J-O parameters [17, 18], which are a function of crystal field parameters. The band intensities are defined by the line strength (S), in the absorption spectra of different sample. The J-O theory has been proved to be quite successful for the intensity analysis of the spectra of trivalent rare earth ions. Line strength (S_{cal}) of an electric dipole transition between initial J manifold $|f^N(\alpha, S, L)J>|$ and terminal J′ manifold $|f^N(\alpha', S', L')J'>|$ is given by

$S_{cal} = \sum_{\lambda=2,4,6} \Omega_\lambda |f^N(\alpha, S, L)J>|\|U^\lambda\||f^N(\alpha', S', L')J'>|^2$

where $|f^N(\alpha, S. L)J>|$ are the basis states in the LS coupling scheme and α represent an extra quantum number that might be necessary to describe the states completely, U^λ are the unit tensor operators of rank λ' which are double reduced to yield the matrix elements $<\|U^\lambda\|>$ in the intermediate coupling [19], and Ω_λ are the phenomenological J-O intensity parameters

The main outcome of composition on Ω_λ values arises through their dependence on the odd order terms in the expansion of local field at the RE site. Small highly charged ions polarize the neighboring oxygen ions more strongly, which in turn, increase the field at the RE ions. These J-O parameters are computed for ZnO:Nd^{3+} nanoparticle in Table 3.

Table 3. J-O intensity parameters (Ω) for Nd^{3+} ion doped ZnO nanoparticles

Ω parameters	Nd^{3+} doping in ZnO nanoparticle		
	0.1 mol%	0.2 mol%	0.3 mol%
Ω_2 (10^{-20})	3.66	3.40	1.25
Ω_4 (10^{-20})	4.19	5.67	8.32
Ω_6 (10^{-20})	8.27	4.04	8.34
Ω_4/Ω_6	0.50	1.40	0.99

These are obtained by using partial regression method [20] taking into consideration of all the observed absorption peaks. These considerations show the general tendency of $\Omega_2 < \Omega_4 < \Omega_6$. The small values of Ω_2's in the specimen may be associated with the micro-structural homogeneity around the Nd^{3+} ions. $\Omega_2 < 2.0$ indicates lesser degree of covalence in ZnO:Nd^{3+} nano-ion. J-O theory has been used to interpret the spectral intensity (line strength S_{exp}) of absorption levels. The Ω_λ parameters are very important since they are used in the calculation of laser parameters. Ω_2 parameter involves the long range terms in the crystal field potential and is most sensitive [21-23] to the native physical deviations.

Energy Parameters. The values of Slater-Condon parameters (F_k), Lande′ parameters (ζ_{4f}) and Racah parameters (E^k) for the free ions as well as the doped ZnO:Nd^{3+} nano-ions have been given in Table 4. For all the cases, the relation among F_k parameters are found to be $F_2 > F_4 > F_6$.

Table 4. Computed values of Slater-Condon parameter (F_k), Lande′ parameter (ζ_{4f}), Racah parameter (E^k), Nephelauxetic ratio (β′) and Bonding parameter ($b^{1/2}$) for Nd^{3+} doped ZnO nanomaterial

Parameters	Free ions	Nd^{3+} doping in ZnO nanoparticle		
		0.1 mol%	0.1 mol%	0.1 mol%
F_2 (cm^{-1})	331.09	330.15	340.86	335.63
F_4 (cm^{-1})	50.72	49.33	43.22	51.99
F_6 (cm^{-1})	5.15	5.00	5.72	5.04
ζ_{4F} (cm^{-1})	884.00	890.79	895.595	882.24
E^1 (cm^{-1})	5024.00	5011.75	5033.51	5004.12
E^2 (cm^{-1})	23.90	24.57	24.91	24.99
E^3 (cm^{-1})	497.00	482.86	480.85	483.90
F_4 / F_2	0.15	0.17	0.12	0.17
F_6 / F_2	0.02	.02	0.01	0.013
E^1 / E^3	10.11	10.50	10.46	9.674724
E^2 / E^3	0.05	0.08	0.05	0.05
β’	…	0.991	0.9291	0.8746
$b^{1/2}$	…	0.04	0.02	0.025

Calculated values of F_4/F_2 ~ 0.12-0.17 and F_6/F_2 ~0.01-0.013 are nearly same as the reported values. The value of ζ_{4f} parameters are ~ 890.79, 895.59 and 882.24 for 0.1 mol%, 0.2 mol% and 0.3 mol% of Nd^{3+} ion doped ZnO nanomaterial. It is of the same order as observed for free ions. However, the calculated value of ζ_{4f} by Blume et.al [24] is ~1130cm^{-1}. The higher calculated value may be due to use of analytical non-relativistic Hartree-Fock functions of f-orbital. It may be pointed out that ζ_{4f} values are higher than the corresponding Pr^{3+} ions. Further the change in ζ_{4f} values on doping Nd^{3+} is larger than the corresponding F_k values. This suggests that the ligands affect spin-orbit coupling more than the electrostatic repulsion.
The values of Racah parameters E^1, E^2 and E^3 have been calculated by the F_k parameters. The ratio of E^1/E^3 ~ 9.67-10.50 and E^2/E^3 ~ 0.050-0.08 are found to remain almost constant over the entire range of Nd^{3+} ion doping concentrations and are in good approximation with the corresponding hydrogenic ratios [25]. Using F_k parameters, Nephlauxetic ratio (β′) and bonding parameter ($b^{1/2}$) are obtained in the range of 0.8746-0.9291 and 0.02-0.04 respectively. The order of the bonding parameters in different concentration of the nano-specimens are 0.1 mol% > 0.2 mol% > 0.3 mol%.

Fluorescence Spectra. The fluorescence spectra of ZnO:Nd^{3+} nanoparticle have been recorded and shown in Fig. 8 and Fig. 9 respectively for the wavelength range 600-900 nm and 1000-1500 nm respectively. The vertical axis in Fig. 8 and Fig. 9 represents intensity in arbitrary units (a.u.). The excitation of the Nd^{3+} ions is done by the radiations (optical pumping) corresponding to its intense absorption bands. The wavelength of exciting radiation is written on each spectrum. Observed values of wavelength (λ) and half bandwidth ($\Delta\lambda_{eff}$) at 583 nm excitation wavelength for various fluorescence peaks of Nd^{3+} doped ZnO nanomaterial with different doping concentrations have been given in Table 5.

Radiative Properties. The radiative properties of uncommon soil ions have been theoretically studied by Krupke [26, 27] and others [28] in relation to J-O intensity parameters in absorption spectra. These properties are often called laser parameters [29]. For investigating signifyable laser transitions, σ_P is an important parameter. It is also found to be an implicative measure of the rate of energy extraction from the optical material. Large value of σ_P is advantageous for a short threshold and high improvement in the laser transition process.

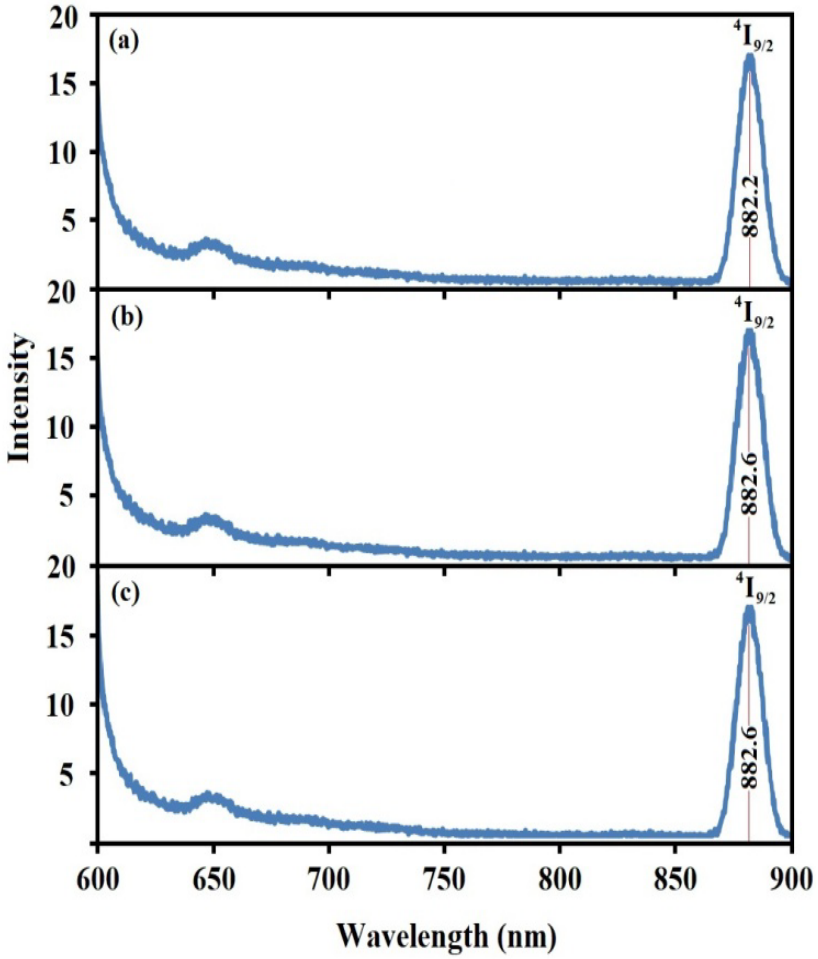

Fig. 8. Fluorescence spectrum of ZnO nanomaterial doped with (a) 0.1 mol %, (b) 0.2 mol % and (c) 0.3 mol % of Nd^3 ions for 600-900 nm wavelength range

Table 5. Observed values of wavelength (λ) and half bandwidth ($\Delta\lambda_{eff}$) for various fluorescence peaks of Nd^{3+} doped ZnO nanomaterial with different doping concentrations at 583 nm excitation wavelength

Transition levels	**Nd^{3+} doping concentration in ZnO nanomaterial**	**λ (nm)**	**$\Delta\lambda_{eff}$ (nm)**
$^4F_{3/2} \rightarrow {}^4I_{9/2}$	0.1 mol%	882.2	13.4
	0.2 mol%	882.6	13.0
	0.3 mol%	882.6	12.6
$^4F_{3/2} \rightarrow {}^4I_{11/2}$	0.1 mol%	1046.0	100
	0.2 mol%	1047.0	100
	0.3 mol%	1048.0	100
$^4F_{3/2} \rightarrow {}^4I_{13/2}$	0.1 mol%	1380.0	100
	0.2 mol%	1380.0	100
	0.3 mol%	1383.0	100
$^4F_{3/2} \rightarrow {}^4I_{15/2}$	0.1 mol%	1403.0	200
	0.2 mol%	1405.0	300
	0.3 mol%	1408.0	100

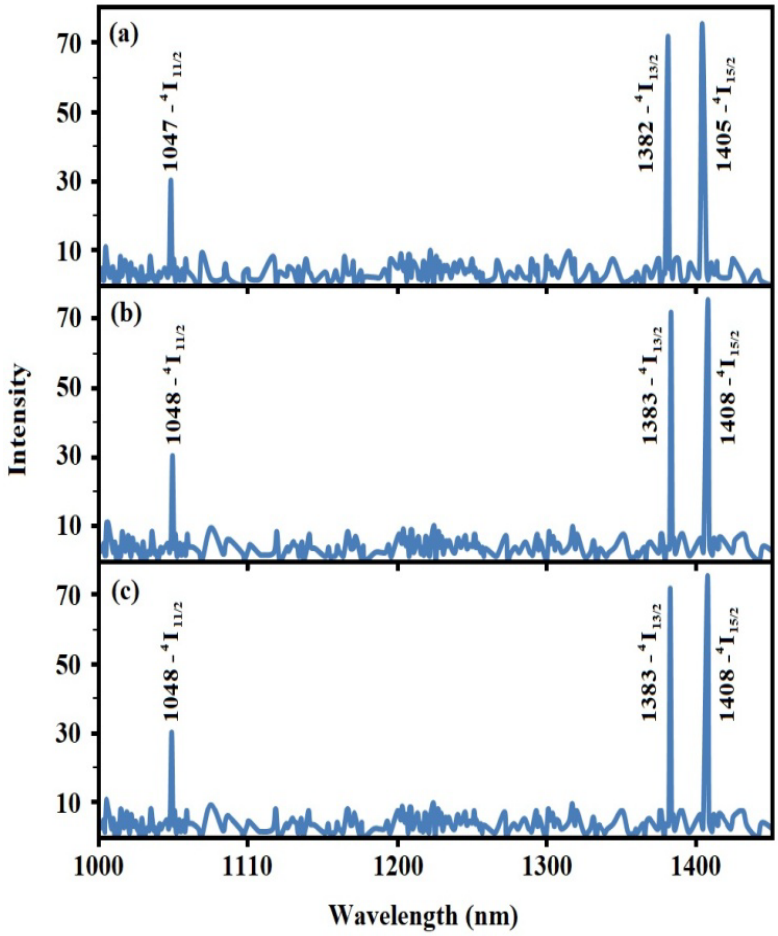

Fig. 9. Fluorescence spectrum of ZnO nanomaterial doped with (a) 0.1 mol %, (b) 0.2 mol % and (c) 0.3 mol % of Nd^{3+} ions for 1000-1500 nm wavelength range

Different laser factors like emission probability A, branching ratio β, radiative life time τ, and stimulated emission cross-section σ_P for the Nd^{3+} ion doped ZnO nanomaterial specimens are given in Table 6 by using the emission wavelength, reduced matrix elements for the relevant transitions and the J-O parameters, Ω_2, Ω_4 and Ω_6.

Table 6. Observed values of spontaneous emission probability (A), fluorescence branching ratio (β), radiative time (τ) and emission cross section (σ_p) for various fluorescence peaks of Nd^{3+} doped ZnO nanomaterial with different doping concentrations at 583 nm excitation wavelength

Transition levels	**Nd^{3+} doping concentration in ZnO nanomaterial**	***A*** **(s^{-1})**	***β***	***τ*** **(μs)**	***σ_p*** **(10^{-20}) cm^2**
$^4F_{3/2} \rightarrow {}^4I_{9/2}$	0.1 mol%	1.91	1.00	523.00	1.39
	0.2 mol%	1.23	5.15	813.00	1.73
	0.3 mol%	1.91	4.40	376.00	2.80
$^4F_{3/2} \rightarrow {}^4I_{11/2}$	0.1 mol%	2.01	0.51	498.00	20.10
	0.2 mol%	1.08	0.42	929.00	2.32
	0.3 mol%	2.00	0.46	501.00	6.47
$^4F_{3/2} \rightarrow {}^4I_{13/2}$	0.1 mol%	0.40	0.09	245.00	10.32
	0.2 mol%	0.19	0.09	509.00	1.28
	0.3 mol%	0.40	0.09	247.00	3.97
$^4F_{3/2} \rightarrow {}^4I_{15/2}$	0.1 mol%	0.26	0.05	372.00	10.86
	0.2 mol%	0.001	0.06	771.00	2.15
	0.3 mol%	0.002	0.06	376.00	2.80

As the 4f orbital of the tri-positive Nd ion are very efficiently shielded by 5s and 5p orbital, the peak values of fluorescence bands are not affected much by the host matrix in the NIR region. Four fluorescence bands have been observed in ZnO nanomaterial doped with 0.1 mol %, 0.2 mol % and 0.3 mol % of Nd^{3+} ions. They have been assigned to transitions $^4F_{3/2} \rightarrow {}^4I_{9/2}$, $^4F_{3/2} \rightarrow {}^4I_{11/2}$, $^4F_{3/2} \rightarrow {}^4I_{13/2}$ and $^4F_{3/2} \rightarrow {}^4I_{15/2}$.The spontaneous emission probability (A) values have been calculated for the fluorescence bands at 882.2 nm ($^4F_{3/2} \rightarrow {}^4I_{9/2}$), 1046 nm ($^4F_{3/2} \rightarrow {}^4I_{11/2}$), 1380 nm ($^4F_{3/2} \rightarrow {}^4I_{13/2}$) and 1403 nm ($^4F_{3/2} \rightarrow {}^4I_{15/2}$) for 0.1 mol %, 0.2 mol % and 0.3 mol % of Nd^3 ion doped ZnO nanomaterials (Table 5). A value is found to be maximum for $^4F_{3/2} \rightarrow {}^4I_{13/2}$ transition for all the observed dopant concentrations of Nd^{3+} ions. These values for the other transitions are comparatively small.

The obtained results indicate that the $^4F_{3/2} \rightarrow {}^4I_{11/2}$, $^4F_{3/2} \rightarrow {}^4I_{13/2}$ and $^4F_{3/2} \rightarrow {}^4I_{15/2}$ can be considered as the most probable transitions for all the Nd doped ZnO nanomaterial specimens, suggesting that, these transitions can be used as a good laser transition. The radiative life time τ for a transition is reciprocal of spontaneous emission probability A. These values of τ are given in Table 5 for 0.1 mol %, 0.2 mol % and 0.3 mol % of Nd^3 ion doped ZnO nanomaterials. The minimum τ values have been obtained for $^4F_{3/2} \rightarrow {}^4I_{13/2}$ and $^4F_{3/2} \rightarrow {}^4I_{11/2}$ transitions in comparison to two others transitions. The stimulated emission cross-sections, σ_p are calculated using the observed peak values λ_p of the fluorescence, their effective line width $\Delta\lambda_{eff}$ (Table 4) and the A values (Table 5). The σ_p parameter is the most important parameter as per the radiative properties are concerned. Its value (Table 5) signifies the rate of energy extraction from the laser material and is generally used to predict laser action in RE doped material prepared on laboratory scale.

Discussion

This synthesis and study of the ZnO doped with 0.1 mol%, 0.2 mol% and 0.3 mol % Nd^{3+} ion describes the fluorescence spectra of the ZnO:Nd^{3+} nanomaterial at room temperature. The SEM images of the ZnO:Nd^{3+} nanomaterial demonstrates clearly the structural formation of the ZnO:Nd^{3+} nanoparticles, and change of the morphology of the nanoparticles with the different concentration of Nd^{3+} ions. From the TEM images of the ZnO:Nd^{3+} nanomaterial it is obvious that with the increase in concentration of Nd^{3+} ions, the particle size decreases. Consideration of all the observed absorption peaks show the general tendency of $\Omega_2 < \Omega_4 < \Omega_6$. The small values of Ω_2's in the specimen may be associated with the micro-structural homogeneity around the Nd^{3+} ions. $\Omega_2 <$ 2.0 indicates lesser degree of covalence in ZnO:Nd^{3+} nano ion. The study of the radiative properties of the ZnO:Nd^{3+} nanomaterial suggests that the most probable laser transitions in different ZnO:Nd^{3+} specimens are $^4F_{3/2} \rightarrow {}^4I_{11/2}$, $^4F_{3/2} \rightarrow {}^4I_{13/2}$ and $^4F_{3/2} \rightarrow {}^4I_{15/2}$.

Conclusion

From this study, it can be concluded that 0.3mol% concentration of $Nd3^+$ ion doping in ZnO will become most suitable for its optical properties by altering its electronic structure enhancement in different optoelectronic efficiencies application. The ZnO size growth inhibition phase reduction narrow down the band gap and reduces agglomerations in chemical medium. Aimed at all the ZnO:Nd^{3+} nanoparticle specimen, suggesting that, transitions $^4F_{3/2} \rightarrow {}^4I_{11/2}$, $^4F_{3/2} \rightarrow {}^4I_{13/2}$ and $^4F_{3/2} \rightarrow {}^4I_{15/}$ can be used as a laser transition. Nd is individual of the record broadly jumble-sale essentials for great control laser applications.

Also, Nd^{3+} incapacitating shrinks the band gap energy and develops the option of the photo degradation of organic dyes. ZnO thin film exhibits high photocatalytic performance under UV-irradiation of methylene blue. In addition, the low toxicity and strong UV-radiation absorption ability of ZnO nanoparticles further enhance their attractiveness as an antibacterial agent [30]. Hence, the RE component drugged ZnO:Nd^{3+} nanoparticle finds numerous attractive possessions in optoelectronic and spintronic uses.

Acknowledgements

Acknowledgements are due to Institute Instrumentation Centre (IIC), IIT Roorkee for providing facilities for recording FL spectra, absorption spectra, SEM and TEM imageries of the sample. Thanks are due to Prof. Ramesh Chandra, Head, IIC, IIT Roorkee for his valuable help in this study. One of the author (S. Pal) is thankful to Dr. J. P. Prasad for providing her the required facilities. Thanks are also due to Department of Physics, J. N. V. University Jodhpur, Rajasthan and Biotech Department, GB Pant Agriculture University, Pantnagar respectively for providing XRD spectra and FTIR spectra of the sample.

References

[1] S. Li, L. Zhou, H. Zhang, Investigation progresses of rare earth complexes as emitters or sensitizers in organic light-emitting diodes, Light Sci Appl., 11 (2022) 177.

[2] L. U. Khan, Z. U. Khan, Rare Earth Luminescence: Electronic Spectroscopy and Applications. In: Sharma, S. (eds) Handbook of Materials Characterization. Springer, Cham. (2018) 345-404 https://doi.org/10.1007/978-3-319-92955-2_10.

[3] A. M. Konstantinidis, E. A. Lalla, G. Lopez-Reyes, U. R. Rodríguez-Mendoza, E.A. Lymer, J. Freemantle, M. G. Daly, Statistical learning for the estimation of Judd-Ofelt parameters: A case study of Er3+: Doped tellurite glasses, Journal of Luminescence, 235 (2021) 118020.

[4] S. Shukla, D. K. Sharma, A review on rare earth (Ce and Er)-doped zinc oxide nanostructures, Materials Today: Proceedings, 34(3) (2021) 793-801.

[5] S. Kumar, P. D. Sahare, Nd-doped ZnO as a multifunctional nanomaterial, Journal of Rare Earths. 30 (2012) 761-768.

[6] J. P. Singh, S. Pal, Y. K. Sharma, A. Nag, Nd-doped CdS nano-particles: Optical band gap and Urbach energy investigations, Journal of Optics, 2024, https://doi.org/10.1007/s12596-024-01746-9.

[7] J. Urban, S. K. Haram, S. W. Gosavi, S. K. Kulkarni, Synthesis and analysis of ZnO and CdSe nanoparticles, Pramana. 65 (2005) 615-620.

[8] U. Koch, A. Fojtik, H. Weller, A. Englein, Photochemistry of semiconductor colloids. Preparation of extremely small ZnO particles, fluorescence phenomena and size quantization effects, Chem. Phys. Lett. 122 (1985) 507-510.

[9] S. Pal, Y. K. Sharma, Spectral, Structural and Characterization of Neodymium Ions Doped Zinc Oxide Nanomaterial, American Journal of Nanoscience. 7 (2021) 49-53.

[10] K. S. Shukla, E. S. Agorku, H. Mittal, A. K. Mishra, Synthesis, characterization and photoluminescence properties of Ce3+-doped ZnO-nanophosphors, Chemical Papers. 68 (2014) 217-222.

[11] B. J. Chen, X. W. Sun, C. X. Xu, B. K. Tay, Growth and characterization of zinc oxide nano/micro-fibers by thermal chemical reactions and vapor transport deposition in air, Physica E: Low-dimensional Systems and Nanostructures. 21 (2004) 103-107.

[12] Y. K. Sharma, J. P. Singh, S. Pal, A. Nag, Fluorescence Study of Pr3+ doped CdS nanoparticles and its Applications in Sensors and Detectors, Journal of Fluorescence. 34 (2024) 915-923.

[13] R. R. Jacobs, M. J. Weber, Dependence of the 4F3/2 → 4I11/2 Induced-Emission Cross Section for Nd3+ on Glass Composition, IEEE J. Quantum Electron. 12 (1976) 102.

[14] P. X. Gao, Z. L. Wang, Nanopropeller arrays of zinc oxide, Appl. Phys. Lett. 84 (2004) 2883-2885.

[15] S. Boruah, S. Mustafiza, D. Saikia, J. H. Saikia, P. P. Saikia, K. M. Baruah, Synthesis of ZnO Nanoparticles from Zinc Formate and Their Optical Properties, American Chemical Science Journal. 11 (2016) 1-10.

[16] E. A. Lalla, M. Konstantinidis, I. De Souza, M. G. Daly, I. R. Martín, V. Lavín, U. R. Rodríguez-Mendoza, Judd-Ofelt parameters of RE3+-doped fluorotellurite glass (RE3+= Pr3+, Nd3+, Sm3+, Tb3+, Dy3+, Ho3+, Er3+, and Tm3+), Journal of Alloys and Compounds. 845 (2020) 156028.

[17] B. R. Judd, Optical Absorption Intensities of Rare-Earth Ions, Phys. Rev. 127 (1962) 750.

[18] G. S. Ofelt, Intensities of Crystal Spectra of Rare-Earth Ions, J. Chem. Phys. 37 (1962) 511-520.

[19] P. Goyal, Y K. Sharma, S. Pal, U. C. Bind, Shu-Chi Huang, Shyan-Lung Chang, The effect of SiO2 Content on structural, physical and spectroscopic properties of Er3+doped B2O3-SiO2-Na2O-PbO-ZnO Glass system, J. Non-cryst Solids. 463 (2017) 118-127.

[20] W. Luo, J. Liao, R. Li, X. Chen, Determination of Judd-Ofelt Intensity Parameters from the Excitation Spectra for Rare-Earth Doped Luminescent Materials, Physical chemistry chemical physics, 12 (13) (2010) 3276-3282.

[21] P. Psuja, D. Hreniak, W. Strek, Rare-Earth Doped Nanocrystalline Phosphors for Field Emission Displays, Journal of Nanomaterials. (2007).

[22] K. Sahu, A. Ali, A. K. Kar, Altering the Photoluminescence Emission Quenching and Energy Transfer for the Photocatalytic Behaviour of ZnO Nanostructures, ECS Journal of Solid State Science and Technology. 11 (2022) 086003.

[23] N. Joudeh, D. Linke, Nanoparticle classification, physicochemical properties, characterization, and applications: a comprehensive review for biologists, J Nanobiotechnol. 20 (2022) 262.

[24] M. Blume, A. J. Freemen, R. E. Watson, Theory of Spin-Orbit Coupling in Atoms. III, Physical Review A, 134 (1964) A320.

[25] G. H. Dieke, Spectra and Energy Levels of Rare Earth Ions in Crystals, in: H. M. Crosswhite, H. Crosswhite (Eds.), Interscience Publishers, New York, 1968.

[26] W. F. Krupke, Radiative transition probabilities within the 4f3 ground configuration of Nd:YAG, J. Quantum Electron. 7 (1971) 153.

[27] W. F. Krupke, Induced Emission Cross Sections in Neodymium Laser Glasses, IEEE J. Quantum Electron. 10 (1974) 450-457.

[28] R. Balda, J. Fernandez, A. Mendioroz, J. L. Adams, B. Boulard, Temperature-dependent concentration quenching of Nd3+ fluorescence in fluoride glasses, J. Phys.: Condens. Matter. 6 (1994) 913.

[29] B. Denker, P. Fjodorow, M. Frolov, B. Galagan, V. Koltashev, V. Plotnichenko, M. Sukhanov, S. Sverchkov, A. Velmuzhov, Rare-Earth-Doped Selenide Glasses as Laser Materials for the 5–6 μm Spectral Range, Photonics. 10 (2023) 1323.

[30] D. Sharma, J. Rajput, B. S. Kaith, M. Kaur, S. Sharma, Synthesis of ZnO nanoparticles and study of their antibacterial and antifungal properties, Thin Solid films. 519 (2010) 1224.